

Few-Shot Semantic Segmentation Augmented with Image-Level Weak Annotations

Shuo Lei Xuchao Zhang Jianfeng He Fanglan Chen Chang-Tien Lu

Department of Computer Science, Virginia Tech, Falls Church, VA, 22043

{slei, xuczhang, jianfenghe, fanglanc, ctlu}@vt.edu

Abstract

Despite the great progress made by deep neural networks in the semantic segmentation task, traditional neural-network-based methods typically suffer from a shortage of large amounts of pixel-level annotations. Recent progress in few-shot semantic segmentation tackles the issue by utilizing only a few pixel-level annotated examples. However, these few-shot approaches cannot easily be applied to utilize image-level weak annotations, which can easily be obtained and considerably improve performance in the semantic segmentation task. In this paper, we advance the few-shot segmentation paradigm towards a scenario where image-level annotations are available to help the training process of a few pixel-level annotations. Specifically, we propose a new framework to learn the class prototype representation in the metric space by integrating image-level annotations. Furthermore, a soft masked average pooling strategy is designed to handle distractions in image-level annotations. Extensive empirical results on PASCAL-5ⁱ show that our method can achieve 5.1% and 8.2% increases of mIoU score for one-shot settings with pixel-level and scribble annotations, respectively.

1. Introduction

Semantic segmentation, one of the most challenging tasks in computer vision, aims to assign a categorical label to each pixel of an image according to its enclosing object or region. In the past few years, a number of deep-neural-network-based approaches such as FCN [15], DeepLab [1] and PSPNet [35] have been proposed for the semantic segmentation task. However, these approaches typically require large-scale pixel-level annotations for training their model parameters, which are expensive to obtain. Some weakly- and semi-supervised segmentation models were proposed to reduce the dependence on pixel-level annotated data but still suffer from the issue of model generalization, which makes them hard to be applied to unseen categories.

Recently, there has been increasing interest in the study of few-shot learning [30, 5, 6, 27], which is learning a novel concept with a few labeled examples, mostly focusing on the image classification task. The purpose of the few-shot segmentation problem is to learn a model that can perform segmentation on novel classes with only a few pixel-level annotated images. Existing studies [3, 31, 33] on few-shot segmentation are based on meta learning, where the model learns a metric space across different training tasks to employ segmentation on new classes with similarity measurements, like distance-based or deep metric-based methods. However, the current setup of each episode is different from how humans learn new concepts in many dimensions, which may limit the learning ability of the model. For instance, by showing a few annotated examples and a set of unlabeled images that contain the target object, even if the location of the target object in the image is not specified, humans are still capable of inferring various forms of a new concept and learning some extra knowledge from these unlabeled images.

To better mimic human learning behaviors, we consider a new scenario where the segmentation of novel classes are learned in the combination of pixel- and image-level annotations, which is shown in Figure 1. Specifically, in a N -way K -shot segmentation task, we aim to perform segmentation on the query images with K pixel-level and L image-level annotated images from each of the N classes. It is worth emphasizing that mixing strong (pixel-level) and weak (image-level) annotations is a widely used setting to improve the model performance in the existing semantic segmentation works [19, 8, 16, 28]. But this paper is the first time to consider doing so in the few-shot segmentation task. Such image-level labeled images could be obtained from crowd-sourcing or existing public image datasets like ImageNet [23]. In many cases, it may be much easier for a human to determine the existence of the target object in the image than making a pixel-level annotation.

To the best of our knowledge, our proposed approach is the first few-shot semantic segmentation model that can integrate weak image-level annotations into traditional pixel-

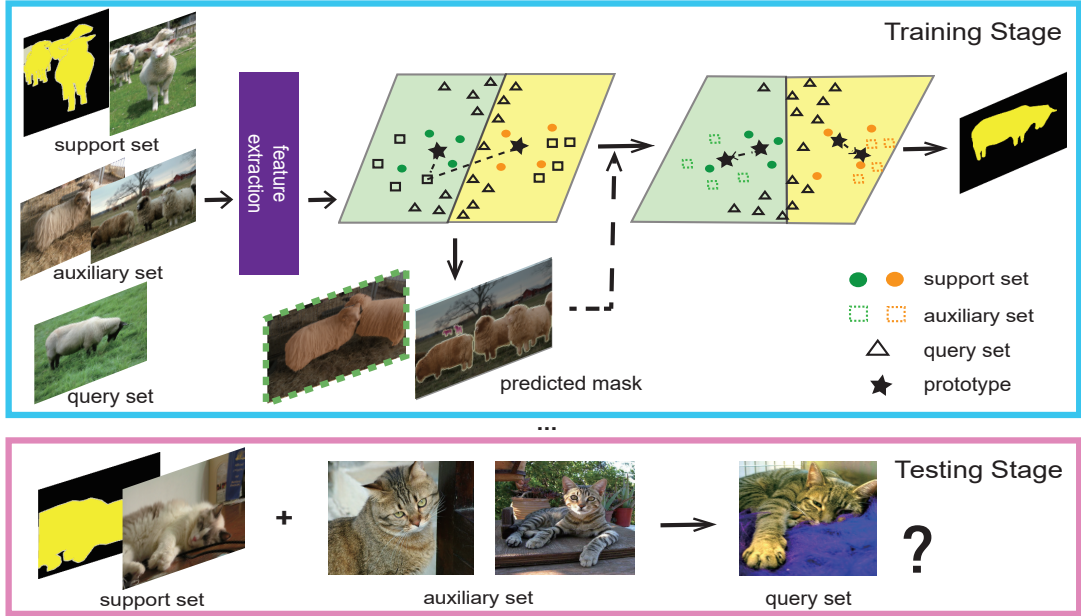


Figure 1. Illustration of a 1-way 1-shot with 2 image-level auxiliary images semantic segmentation task. Our objective is to optimize the class representation in the metric space by using image-level labeled data. FSIL first maps the support, auxiliary, and query images into embedding features and extracts the original prototype from the support set (circles, rectangles, and triangles, respectively). Then it segments the image-level labeled images via original prototypes and re-feeds the embedding features of pixels with high prediction confidence into the prototype extraction. The integrated prototypes are obtained by incorporating those weak annotation images.

level labels. It is nontrivial to consider both pixel-level and image-level labels simultaneously in the few-shot semantic segmentation task because of 1) the discrepancies between pixel-level segmentation labels and image-level weak annotation; and 2) the distraction of segmentation object in image-level annotations. To tackle the above issues, we propose a few-shot semantic segmentation model augmented with image-level labels (FSIL), as shown in Figure 1. To sum up, our main contributions are as follows: We first propose a class prototype augmentation method to learn the prototype representation in the metric space by utilizing image-level annotations. Moreover, we propose a soft-masked average pooling strategy for enhanced prototype generation to handle distraction in image-level annotation. In addition, extensive empirical results on PASCAL-5ⁱ show that our FSIL method can achieve 5.1% and 8.2% increases in mIoU score for one-shot settings with pixel-level and scribble annotations, respectively.

The remainder of this paper is organized as follows. Section 2 reviews related work in the few-shot semantic segmentation and weakly-supervised segmentation categories. Section 3 provides a formal problem formulation. The proposed FSIL model is presented in Section 4. In Section 5, the experimental results are analyzed and the paper concludes with a summary of our work in Section 6.

2. Related Work

The prior work related to this paper is summarized below in the categories of semi- and weakly-supervised segmentation, few-shot learning and few-shot semantic segmentation.

2.1. Semi-supervised and Weakly-supervised Segmentation

In light of the expensive cost of annotated pixel-level labels, the segmentation task has recently received increasing interest in the semi- and weakly-supervised training schemes. Weakly-supervised methods aim to use weak labels like image-level class labels [19, 32] and bounding boxes [2, 12] to train the segmentation model, achieving the similar performance as supervised models. And the general idea of existing work [28, 10, 17] on the semi-supervised segmentation task is to employ a GAN-based method that learns the distribution of images and generate additional images to improve the performance of the segmentation network. However, these approaches still require large training sets, which limits their widespread use in real applications.

2.2. Few-shot Learning

Few-shot learning aims to learn general knowledge that can be applied to learn a novel class with a few examples. Most of the proposed methods are deep meta-learning mod-

els, which try to optimize the base learner using learning experiences from multiple similar tasks. One class of existing methods for few-shot learning is gradient-based methods, which aim to adapt the model to a novel class within a few fine-tuning updates [5, 6, 11]. The typical model in this class is MAML [5] which learns the initial parameters of the base learner to make the model fast adapt to a novel task. Finn et al. [6] extends it with a probabilistic algorithm to train with variational approximation. Another class of few-shot learning approaches is metric learning, which is learning a metric space across different tasks [13, 30, 27]. Prototypical Network [27] takes an average over all sample embedding to present each class and performs nearest-neighbor matching to classify data. Relation Network [29] replaces distance-based prediction with a learning relation module to compare the relation between each class.

2.3. Few-shot Semantic Segmentation

The few-shot semantic segmentation task is first solved by using the support branch to predict the weights of the last layer in the query branch [24]. AMP [25] adopts a similar idea in which the convolutional filters of the final query segmentation layer are imprinted by the embedding of the support set. Most of the existing approaches on few-shot semantic segmentation are proposed based on metric learning methods [3, 33, 31, 18]. CANet [33] employs the same embedding module for both the support and query sets, and it learns a dense comparison module to a segment. Prototype learning-based methods are performed on the few-shot segmentation problem [3, 31]. PANet [31] takes the averaged feature embedding in a pixel-level as the class prototype and trains the metric space with prototype alignment constraints between support and query prototypes.

3. Problem Setting

Our purpose is that a model trained on a large labeled dataset \mathcal{D}_{train} can make a segmentation prediction on a testing dataset \mathcal{D}_{test} with a few annotated examples. The class set \mathcal{C}_{train} in \mathcal{D}_{train} has no overlap with \mathcal{D}_{test} , i.e., $\mathcal{C}_{test} \cap \mathcal{C}_{train} = \emptyset$. Following previous work [31, 33], we adopted an episodic paradigm in the few-shot segmentation task. In particular, given an N -way, K -shot task, a set of episodic \mathcal{T}_{train} and \mathcal{T}_{test} are sampled from \mathcal{D}_{train} and \mathcal{D}_{test} , respectively. Each episode e is composed by 1) a *support* set $\mathcal{S}_e = \{(I_i^s, M_i^s)\}_{i=1}^{N \times K}$, containing K (*image, mask*) pairs for each of the N categories in the foreground, where (I_i^s, M_i^s) represents the pair of support image I_i^s and its corresponding binary mask M_i^s for the foreground class, 2) a *query* set $\mathcal{Q}_e = \{(I_j^q, M_j^q)\}_{j=1}^Q$, which contains Q different query sample pairs (I_j^q, M_j^q) from the same N categories, and 3) an *auxiliary* set $\mathcal{A}_e = \{I_t^a\}_{t=1}^{N \times V}$, containing V image-level labeled images I_t^a for each of the same N categories, but no pixel-level annota-

tion is available. The set of all target classes in the foreground for episode e denotes as \mathcal{C}_e , and $|\mathcal{C}_e| = N$. For each episode e , the model is supposed to segment images from \mathcal{Q}_e with the combination of \mathcal{S}_e and \mathcal{A}_e . As each foreground class c contains many pixel-level labeled data pairs and image-level labeled data, the model is trained on different combination-samples avoiding over-fitting.

4. Model

To introduce our model, we first show a global view of the framework. Then we describe the first stage of the model: prototype representation learning. Finally, we introduce the second stage of the model, which contains soft-masked average pooling, distilled soft-masked average pooling, and an iterative fusion module.

4.1. Overall Architecture

We propose a new framework that can solve the few shot segmentation problem with a combination of pixel- and image-level labeled data. The main idea of our model is to learn a better prototype representation of the class by fusing the knowledge from the image-level labeled data. Specifically, the original prototypes are first obtained on the support set and are used to classify these image-level annotated images. The most confidently predicted pixels are added to the support set with the prediction of the original prototypes as the pseudo labels. To this end, we propose a novel prototype fusion strategy that contains the distilled soft-masked average pooling method and iterative fusion module. Figure 2 shows an overview of our model. In particular, for each episode, it first obtains the embedding features of the support, auxiliary, and query images via the feature encoder module. The original prototypes are computed by using masked average pooling over the support feature and mask. Then the Iterative Fusion Module (IFM) segments the image-level labeled images via the original prototypes and re-feeds the embedding features of those image-level labeled features with the proposed distilled soft-masked average pooling method. In the end, we predict the mask of the query image by the fused prototypes obtained from the Iterative Fusion module.

4.2. Prototype Representation Learning

Inspired by Wang et al. [31], we represent each category of segmentation task as a prototype in the metric space. The original class-specific prototypes are obtained by employing masked average pooling over the support set, which averages the features of the pixels only belonging to the support classes, and each pixel of the query image is labeled by its nearest prototypes in the metric space. Thus, the proto-

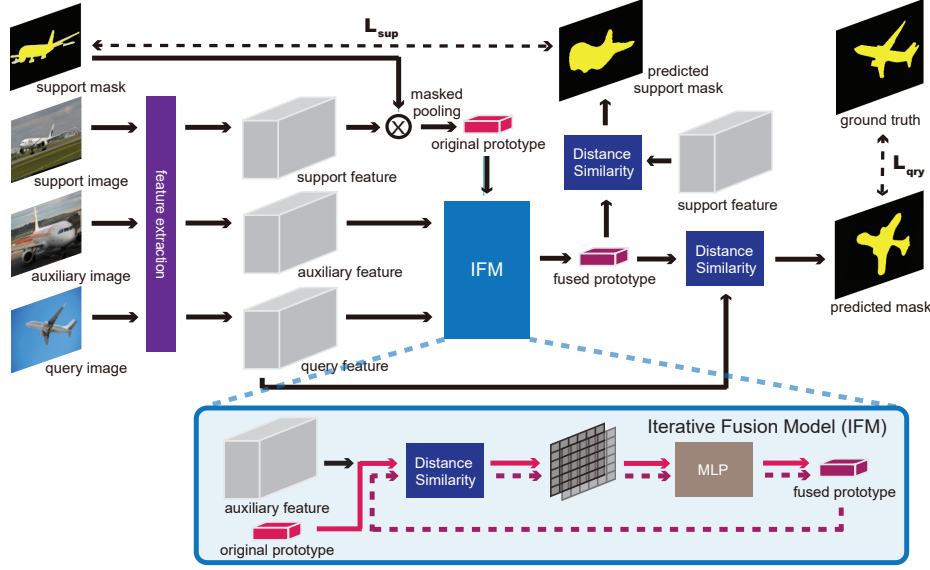


Figure 2. Overview of the proposed network structure. The support, auxiliary, and query images are embedded into deep features via the feature encoder. Then the model employs masked average pooling over the support set to get the original prototypes. Iterative Fusion Module (IFM) segments the image-level labeled images via original prototypes and re-feeds the embedding features of pixels with the proposed distilled soft-masked average pooling. The fused prototypes are obtained via the IFM and are used to segment query images. \mathcal{L}_{sup} and \mathcal{L}_{qry} denote the standard cross entropy loss between the segmentation results and the ground truth of the support set and query set, respectively.

type p_c of the foreground class c is defined as follows:

$$p_c = \frac{1}{|\mathcal{S}_e^c|} \left(\sum_{(I_i^s, M_i^s) \in \mathcal{S}_e^c} \text{MP}(I_i^s, M_i^s) \right), \quad (1)$$

$$\text{where } \text{MP}(I_i^s, M_i^s) = \frac{\sum_{x_j \in I_i^s, y_j \in M_i^s} f(x_j) y_j}{\sum_{y_j \in M_i^s} y_j} \quad (2)$$

where $\mathcal{S}_e^c \subset \mathcal{S}_e$ is the subset of support belonging to class c . We have $I_i^s = \{x_j\}_{j=1}^{w \times h}$ and $M_i^s = \{y_j\}_{j=1}^{w \times h}$, where w and h denote the width and height of the image, respectively. $f(\cdot)$ is defined as a feature encoder function that encodes the image to the feature space and $\text{MP}(\cdot)$ denotes the masked average pooling function. Moreover, the background prototype p_b is computed by averaging all the features of the pixels that do not belong to any foreground class in \mathcal{C}_e .

Accordingly, we obtain a prototype set containing all prototypes for each episode e , i.e., $\mathcal{P}_e = \{p_c | c \in \mathcal{C}_e\} \cup \{p_b\}$. Then we compute the distances between embedding features of each pixel i in the image and \mathcal{P}_e . The probability of i belonging to class c , i.e., \hat{y}_i^c , is formed as follows:

$$\hat{y}_i^c = \frac{\exp(-d(f(x_i), p_c))}{\sum_{p_c \in \mathcal{P}_e} \exp(-d(f(x_i), p_c))}, \quad (3)$$

$$\hat{y}_i = \arg \max_c \hat{y}_i^c, \quad (4)$$

where \hat{y}_i denotes the predicted class label of the pixel i . Following previous work [31], the distance function $d(\cdot)$ is

adopted as the cosine distance multiplying a factor α , and the multiplier α is fixed at 20.

4.3. Prototype Fusion with Soft-masked Average Pooling

Our model enhances the prototypes by extracting more class representation knowledge from the additional image-level annotations. The most intuitive way to incorporate those image-level annotations is to obtain their pseudo masks by employing the segmentation prediction method in Eq.4 and directly adding them into the support set. However, this process may introduce some noise into the support set. Since the original prototypes can be biased due to data scarcity, it may lead to inaccurate prediction results of image-level labeled data. To tackle this issue, we propose a soft-masked pooling method. Instead of assigning the same weight to each pixel belonging to the support class, we give them a partial assignment based on their probability of falling into the class. Pixels with lower predicted confidence would get lower weights preventing them from distracting the original prototypes. Specifically, for each foreground class c , we first compute the predicted probability map $Y_{i,c}^a = \{\hat{y}_j^c\}_{j=1}^{w \times h}$ and pseudo binary mask $M_{i,c}^a = \{z_j\}_{j=1}^{w \times h}$ of I_i^a based on Eq. 3 and Eq. 4, where the indicator z_j is set to 1 if $\hat{y}_j = c$. A pseudo mask set $\mathcal{R}_e = \{(Y_i^a, \hat{M}_i^a)\}_{i=1}^{N \times V}$ is obtained for \mathcal{A}_e . Then, we compute the representative vector by averaging the pixels within the object regions on the feature map. Thus, the soft-masked average pooling can

be formed as:

$$\text{SMP}(I_i^a, Y_i^a, \hat{M}_i^a) = \frac{\sum_{x_j \in I_i^a, \hat{y}_j \in Y_i^a, z_j \in \hat{M}_i^a} f(x_j) \hat{y}_j z_j}{\sum_{\hat{y}_j \in Y_i^a, z_j \in \hat{M}_i^a} \hat{y}_j z_j} \quad (5)$$

In this way, the original prototypes can be enhanced by incorporating partial of image-level labeled samples. The fused prototypes can be computed as follows:

$$\begin{aligned} \tilde{p}_c = \frac{1}{|\mathcal{S}_e^c| + |\mathcal{A}_e^c|} & \left(\sum_{(I_i^s, M_i^s) \in \mathcal{S}_e^c} \text{MP}(I_i^s, M_i^s) \right. \\ & \left. + \sum_{\substack{I_j^a \in \mathcal{A}_e^c, \\ (Y_j^a, \hat{M}_j^a) \in \mathcal{R}_e^c}} \text{SMP}(I_j^a, Y_j^a, \hat{M}_j^a) \right), \end{aligned} \quad (6)$$

where $\mathcal{A}_e^c \subset \mathcal{A}_e$ and $\mathcal{R}_e^c \subset \mathcal{R}_e$ are the subset of auxiliary set and pseudo mask with respect to class c , respectively.

4.4. Prototype Fusion with Distilled Soft-masked Average Pooling

In our problem setting, each image-level labeled image contains at least one foreground class in the episode. Therefore, the categories of referred segmentation mask belong to at least two of the $N + 1$ classes (including the background class), which means there is no distractor in the image-level labeled dataset \mathcal{A}_e . However, when computing the prototype of background class, we treat all pixels not belonging to foreground classes as the same category. That means we cannot guarantee two support sets have similar background class representation even if their foreground classes are the same. Moreover, the image-level annotated images may contain an unseen object that does not show up in the background or does not belong to any foreground class in the support set. For example, in Figure 1, the second image in the auxiliary set has some potted plants in the background, which is never seen in the support set.

Under this circumstance, features of unlabeled pixels could still get a pseudo label with higher confidence even if they are far away from all prototypes in the metric space. So the uncertainty of these unseen objects in images may reduce the accuracy of fused prototypes. To alleviate the issue, we use a filter strategy for each prototype when applying soft-masked average pooling over those unlabeled images, which is called distilled soft-masked average pooling. Inspired by [22], we try to compute a threshold γ_c based on the statistics of the distances between pixels and the prototypes. Specifically, we first compute the distance d_j^c between the prototype p_c and the pixel j , and obtain distance matrix D_i^c of image I_i^a for the prototype p_c , i.e. $D_i^c = \{d_j^c\}_{j=1}^{w \times h}$. Then normalized distance set \tilde{D}^c is obtained by normalizing each distance from the distance set $D^c = \{D_i^c\}_{i=1}^{N \times V}$. Finally, the filter threshold γ_c for the

prototype p_c in each episode e is defined as follows:

$$\gamma_c = \text{MLP}([\min_{i,j}(\tilde{D}_{i,j}^c), \max_{i,j}(\tilde{D}_{i,j}^c), \text{var}_{i,j}(\tilde{D}_{i,j}^c), \text{skew}_{i,j}(\tilde{D}_{i,j}^c), \text{kurt}_{i,j}(\tilde{D}_{i,j}^c)]) \quad (7)$$

For each foreground class c , the distraction indicator τ_i of pixel i can be computed as follows:

$$\tau_i = \begin{cases} 1, & \text{d}(f(x_i), p_c) < \gamma_c, \\ 0, & \text{otherwise.} \end{cases} \quad (8)$$

The indicator $H_i^a = \{\tau_j\}_{j=1}^{w \times h}$ of I_i^a for each N categories is applied to filter some pixels that are not worth considering. The indicator set \mathcal{H}_e is defined as $\mathcal{H}_e = \{H_i^a\}_{i=1}^{N \times V}$. This way, the model is forced to only extract objective class-related pixels instead of considering the whole image which may contain novel object classes in the background. Therefore, the Eq.6 for the fused prototype computation can be updated as follows:

$$\begin{aligned} \tilde{p}_c = \frac{1}{|\mathcal{S}_e^c| + |\mathcal{A}_e^c|} & \left(\sum_{(I_i^s, M_i^s) \in \mathcal{S}_e^c} \text{MP}(I_i^s, M_i^s) \right. \\ & \left. + \sum_{\substack{I_j^a \in \mathcal{A}_e^c, H_j^a \in \mathcal{H}_e^c, \\ (Y_j^a, \hat{M}_j^a) \in \mathcal{R}_e^c}} \text{SMP}(I_j^a, Y_j^a, H_j^a \odot \hat{M}_j^a) \right), \end{aligned} \quad (9)$$

where \odot is the element-wise product between two vectors, and $\mathcal{H}_e^c \subset \mathcal{H}_e$ is the subset of indicator set belonging to class c .

4.5. Iterative Fusion Module

Intuitively, if the knowledge extracted from the image-level annotations in the auxiliary set can improve the performance of our model, we can also utilize the image-level annotated images from the query set. Previous work [33] found that the initial prediction is an important clue about the rough position of the objects. Accordingly, we can update the fused prototype with the image-level annotations from query set as follows:

$$\begin{aligned} \tilde{p}_c = \frac{1}{|\mathcal{S}_e^c| + |\mathcal{A}_e^c| + |\mathcal{Q}_e^c|} & \left(\sum_{(I_i^s, M_i^s) \in \mathcal{S}_e^c} \text{MP}(I_i^s, M_i^s) \right. \\ & + \sum_{\substack{I_j^a \in \mathcal{A}_e^c, H_j^a \in \mathcal{H}_e^c, \\ (Y_j^a, \hat{M}_j^a) \in \mathcal{R}_e^c}} \text{SMP}(I_j^a, Y_j^a, H_j^a \odot \hat{M}_j^a) \\ & \left. + \sum_{\substack{I_k^q \in \mathcal{Q}_e^c, H_k^q \in \mathcal{H}'_e, \\ (Y_k^q, \hat{M}_k^q) \in \mathcal{R}'_e}} \text{SMP}(I_k^q, Y_k^q, H_k^q \odot \hat{M}_k^q) \right) \end{aligned} \quad (10)$$

Here R'_e and \mathcal{H}'_e are the pseudo mask set and indicator set of query set \mathcal{Q} in episode e , respectively. As the original prototypes are inevitably biased due to data scarcity, the confidence of the initial probability maps of those images may not be high enough to be considered. Therefore, we iteratively repeat the refinement for several steps to optimize the fusion prototypes in the Iterative Fusion Module (IFM). This process is shown in Figure 2. In particular, we first compute the probability maps via the original prototypes and re-feeds the embedding features with distilled soft-masked average pooling to the IFM. Then we alternatively use fused prototypes in the last epoch to compute the probability maps.

To avoid diluting the knowledge learned from the support set during IFM, we adopt a similar idea from [31] to compute the \mathcal{L}_{sup} . Different from predicting a segmentation mask on the support image by using the prototypes obtained from the prediction results of the query set, we compute the probability maps of support images and query images via the fused prototypes $\tilde{\mathcal{P}}_e = \{\tilde{p}_c | c \in \mathcal{C}_e\} \cup \{\tilde{p}_b\}$. Then compute \mathcal{L}_{sup} and \mathcal{L}_{qry} by applying the standard cross-entropy function on their probability maps and pixel-level ground truth annotations, respectively. Thus the loss function for training our model is $\mathcal{L} = \mathcal{L}_{\text{sup}} + \mathcal{L}_{\text{qry}}$. This way, the model is forced to learn a consistent embedding space and retain the knowledge from the support set when integrating the prototypes.

5. Experiments

5.1. Setup

5.1.1 Datasets

We evaluate the performance of our model on two common few-shot segmentation datasets: PASCAL-5ⁱ and COCO-20ⁱ. PASCAL-5ⁱ dataset is proposed by Shaban et.al [24] and is created from PASCAL VOC 2012 [4] with SBD [7] augmentation. The 20 categories in PASCAL VOC are evenly divided into 4 splits, each containing 5 categories. We use the rest of the images that do not have segmentation labels but have category information in PASCAL VOC 2012 as the auxiliary set. Similarly, COCO-20ⁱ is built from MS COCO [14] and 80 categories are split into 4 folds. For fair comparison, we adopt the same split strategy as the previous work [31]. As all images in MS COCO have its corresponding segmentation label, we use images in its validation folder as the reliable set. Models are trained on 3 splits and evaluated on the rest one in a cross-validation fashion for both datasets. Following the same scheme for testing [31], we average the results from 5 runs with different random seeds, each run containing 1,000 episodes to get stable results. $N_{\text{query}} = 1$ is used for all experiments.

5.1.2 Evaluation Metric

We adopt two common metrics in the few-shot segmentation task [31, 33, 24] to evaluate the model performance: mean-IoU and binary-IoU. Concretely, mean-IoU calculates the Intersection-over-Union of each class and takes the average IoU over all foreground classes. Binary-IoU ignores the difference between categories and treats all object categories in the support set as one foreground class and averages the IoU of foreground and background. As mean-IoU considers the differences between foreground classes, it can reflect the model performance more accurately than binary-IoU. Thus, we mainly use mean-IoU to report the experiment results.

5.1.3 Implementation details

We adopt a VGG-16 [26] network as the feature extractor following conventions. The first 5 convolutional blocks in VGG-16 are kept for feature extraction and the layers after the 5th convolutional block are removed. To maintain large spatial resolution, the stride of the *maxpool4* layer is equal to 1. The convolutions in the *conv5* block are replaced by dilated convolutions with rates 2 to enlarge the receptive field. For the MLP used in the distilled soft-masked pooling, we use a single hidden layer with 20 hidden units with a tanh non-linearity. For implementation, we use Pytorch [20]. Following previous work [34, 31, 18], we pre-train the CNN on ImageNet [23]. All images are resized to 417×417 and augmented by random horizontal flipping. The network is trained end-to-end by SGD with a learning rate of $1e-3$, momentum of 0.9 and weight decay of $5e-4$. We train the model in 20,000 iterations and the batch size is 1. The learning rate is reduced by 0.1 after 10,000 iterations.

5.2. Comparison with the State-of-the-art Methods

5.2.1 PASCAL

We first compare our model with the state-of-the-art methods on PASCAL-5i dataset in 1-way segmentation. Table 1 shows the results in mean-IoU metric and Table 3 shows the results in binary-IoU metric. For fair comparison, we quote the result produced in VGG for the performance of [18]. Our model outperforms the state-of-the-art methods under both evaluation metrics. Specifically, compared with [31] in the mean-IoU metric, our model achieves an improvement of 5.1% in the 1-way 1-shot task and 2% in the 5-shot task, which means the combination of strong and weak annotated images can improve the performance in the few-shot segmentation task, especially when only one pixel-level annotated image is available.

We also present the results in 2-way 1-shot and 5-shot settings to validate the effectiveness of the model on multi-

Table 1. Mean-IoU of 1-way 1-shot and 5-shot segmentation on PASCAL-5ⁱ.

Methods	1-shot					5-shot				
	split-1	split-2	split-3	split-4	mean	split-1	split-2	split-3	split-4	mean
OSLSM [24]	33.6	55.3	44.9	33.5	40.8	35.9	58.1	42.7	39.1	43.9
co-FCN [21]	36.7	50.6	44.9	32.4	41.1	37.5	50.0	44.1	33.9	41.4
PL [3]	-	-	-	-	42.7	-	-	-	-	43.7
SG-One [34]	40.2	58.4	48.4	38.4	46.3	41.9	58.6	48.6	39.4	47.1
AMP [25]	41.9	50.2	46.7	34.7	43.4	51.8	64.6	59.8	46.5	55.7
FWB [18]	47.0	60.0	52.6	48.3	51.9	48.0	59.4	54.5	48.5	52.6
PANet [31]	42.3	58.0	51.1	41.2	48.1	51.8	64.6	59.8	46.5	55.7
FSIL	49.5	61.6	56.0	45.6	53.2	54.1	63.8	62.3	50.5	57.7

Table 2. Mean-IoU of 2-way 1-shot and 5-shot segmentation on PASCAL-5ⁱ.

Methods	1-shot					5-shot				
	split-1	split-2	split-3	split-4	mean	split-1	split-2	split-3	split-4	mean
SG-One [34]	-	-	-	-	-	-	-	-	-	29.4
PANet [31]	-	-	-	-	45.1	-	-	-	-	53.1
FSIL	47.7	60.0	53.3	46.0	51.8	49.1	60.7	58.6	48.2	54.2

Table 3. Binary-IoU of 1-way 1-shot and 5-shot segmentation on PASCAL-5ⁱ.

Methods	1-shot	5-shot
FG-BG [21]	55.0	-
Fine-tuning [21]	55.1	55.6
OSLSM [24]	61.3	61.5
co-FCN [21]	60.1	60.2
PL [3]	61.2	62.3
A-MCG [9]	61.2	62.2
SG-One [34]	63.9	65.9
AMP [25]	62.2	63.8
PANet [31]	66.5	70.7
FSIL	67.0	71.9

Table 4. Mean-IoU of 1-way 1-shot and 5-shot segmentation on COCO.

Method	mean-IoU	
	1-shot	5-shot
PANet [31]	20.9	29.7
FSIL	23.2	30.4

way few-shot segmentation tasks, as shown in Table 2. Our FSIL model outperforms previous works, especially on the 1-shot setting, surpassing the state-of-the-art method by 6.7%.

Figure 3. Qualitative examples of 2-way 1-shot segmentation on the PASCAL-5ⁱ.

Table 4 shows the evaluation results on the MS COCO dataset. Compared to PASCAL VOC, MS COCO has more object categories, making the differences between two evaluation metrics more significant. Thus, we adopt mean-IoU score to evaluate the performance. Our model outperforms the previous PANet [31], which means that our model is able to extract class-related knowledge from the image-level annotations even if there are more unseen objects in it.

5.2.2 MS COCO.

5.2.3 Qualitative Results.

Fig. 4 shows some qualitative examples of in the 1-way 1-shot settings on PASCAL-5ⁱ and MS COCO. The first two rows in Fig.4 is on PASCAL-5ⁱ and the last two rows is on MS COCO. Furthermore, the qualitative results on 2-way 1-shot are shown in Fig. 3.

5.3. Ablation Study

We implement extensive ablation experiments on the PASCAL-5ⁱ dataset to evaluate the effectiveness of different components in our network by using the mean-IoU metric in the 1-way 1-shot task. In Table 5, we compare our model with two baseline models. The first one does

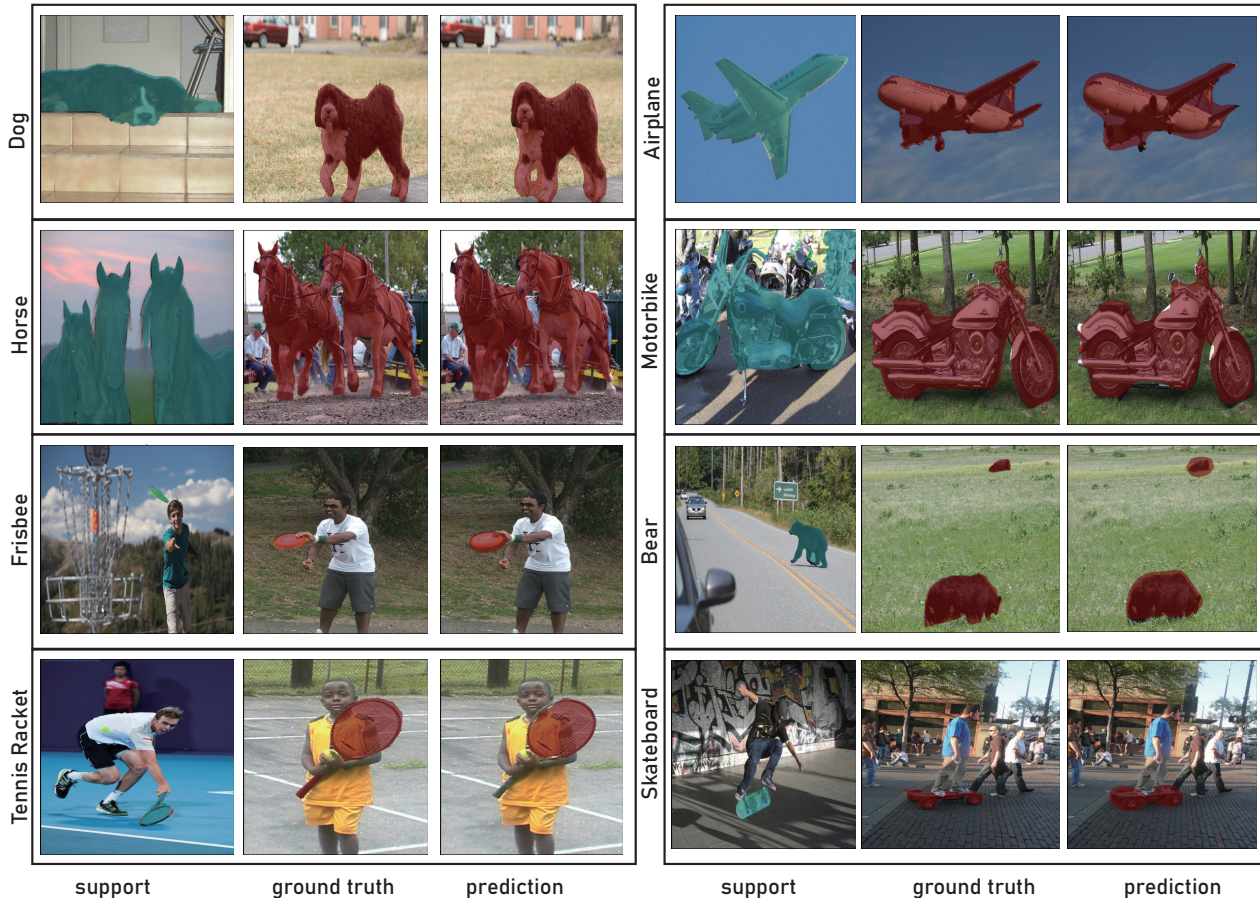


Figure 4. Qualitative examples of 1-way 1-shot segmentation on the PASCAL-5ⁱ and MS COCO. Note that the first two rows are on PASCAL-5ⁱ and the last two rows are on MS COCO.

not adopt the distilled strategy when applying soft-masked pooling (DSMP), which is denoted as FSIL-Smp. The second one does not employ an additional iterative fusion module for the fused prototypes, i.e., the initial prediction from FSIL(FSIL-Init).

Table 5. Ablation study on the choice of proposed module on 1-way 1-shot segmentation task on PASCAL-5ⁱ. The combination of both modules achieves the best performance.

	DSMP	IFM	mean-IoU
FSIL-Smp	✓		51.0
FSIL-Init		✓	52.1
FSIL	✓	✓	53.2

As shown in Table 5, the distilled soft-masked pooling method achieves a 2.2% improvement over the soft-masked pooling method. In addition, the iterative fusion module yields an improvement of 1.1% over the initial prediction. The combination of both modules achieves the best performance.

5.4. Analysis on the Number of Image-Level Annotations

From Fig. 5, we observe the improvements of segmentation performance when the number of image-level annotations increases in both the 1-shot and 5-shot learning. Specifically, the improvement of 1-shot learning is larger than 5-shot learning since the image-level annotations can provide more useful information when the pixel-level annotation is extremely limited. Moreover, we observe that the performance of annotation number 25 is slightly worse than 20 in 5-shot learning. It is mainly caused by the image-level annotations may introduce some distraction into the prototype representation.

5.5. Results on Weak Annotations

We evaluate FSIL with two types of weak annotations: scribble and bounding box. The pixel-level annotations of the support set are replaced by scribbles or bounding boxes. For fair comparison, we use the same annotation generation method proposed in [31]: scribbles are generated from the

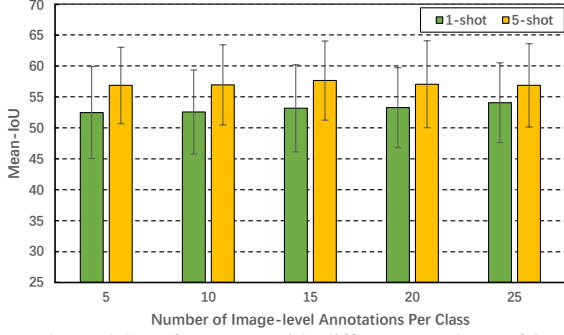


Figure 5. Model performance with different numbers of image-level annotated images.

dense segmentation masks automatically and bounding box is randomly chosen from instance mask.

Table 6. Mean-IoU of using different types of annotations on PASCAL-5ⁱ.

Method	Scribble		Bounding Box		Densed	
	1-shot	5-shot	1-shot	5-shot	1-shot	5-shot
PANet [31]	44.8	54.6	45.1	52.8	48.1	55.7
FSIL	53.0	57.3	51.9	56.2	53.2	57.7

As is shown in Table 6, for scribble annotations, our model achieves significant improvements of 8.2% and 2.7% in 1-shot and 5-shot tasks, respectively. This performance is comparable to the result with an expensive pixel-level annotated support set, which means our model works very well with sparse annotations. In addition, with bounding box annotations, our model significantly outperforms the state-of-the-art methods by 6.8% for the 1-shot task and 3.4% for the 5-shot task. This demonstrates that our model has a greater ability to withstand the noise introduced by the background area within the bounding box. Furthermore, the improvements of the performance in weak annotations validate the robustness of our model. Qualitative results of using scribble and bounding box annotations are shown in Fig. 6.

6. Conclusion

In this paper, a novel weak annotation augmented few-shot segmentation model is proposed to learn a refined prototypes based on both pixel-level segmentation labels and weak image-level annotations. To achieve this, we proposed a new framework to learn the class prototype representation in the metric space with the information of image-level annotations. Moreover, a soft masked average pooling method is designed for handling distraction in image-level weak annotations. Our evaluation results demonstrated the superiority of the proposed method over existing few-shot segmentation models by a significant margin.

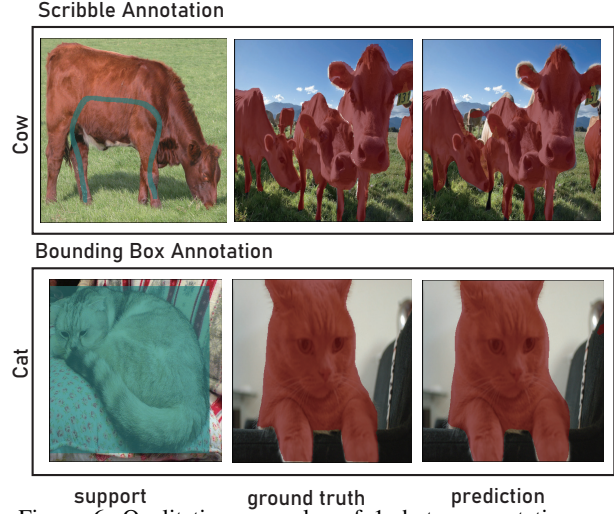


Figure 6. Qualitative examples of 1-shot segmentation on the PASCAL-5ⁱ with weak annotations.

References

- [1] LC Chen, G Papandreou, I Kokkinos, K Murphy, and AL Yuille. Deeplab: Semantic image segmentation with deep convolutional nets, atrous convolution, and fully connected crfs. *IEEE transactions on pattern analysis and machine intelligence*, 40(4):834–848, 2018.
- [2] Jifeng Dai, Kaiming He, and Jian Sun. Boxesup: Exploiting bounding boxes to supervise convolutional networks for semantic segmentation. In *Proceedings of the IEEE International Conference on Computer Vision*, pages 1635–1643, 2015.
- [3] Nanqing Dong and Eric Xing. Few-shot semantic segmentation with prototype learning. In *BMVC*, volume 3, 2018.
- [4] Mark Everingham, Luc Van Gool, Christopher KI Williams, John Winn, and Andrew Zisserman. The pascal visual object classes (voc) challenge. *International journal of computer vision*, 88(2):303–338, 2010.
- [5] Chelsea Finn, Pieter Abbeel, and Sergey Levine. Model-agnostic meta-learning for fast adaptation of deep networks. In *Proceedings of the 34th International Conference on Machine Learning-Volume 70*, pages 1126–1135. JMLR. org, 2017.
- [6] Chelsea Finn, Kelvin Xu, and Sergey Levine. Probabilistic model-agnostic meta-learning. In *Advances in Neural Information Processing Systems*, pages 9516–9527, 2018.
- [7] Bharath Hariharan, Pablo Arbeláez, Lubomir Bourdev, Subhransu Maji, and Jitendra Malik. Semantic contours from inverse detectors. In *2011 International Conference on Computer Vision*, pages 991–998. IEEE, 2011.
- [8] Seunghoon Hong, Hyeonwoo Noh, and Bohyung Han. Decoupled deep neural network for semi-supervised semantic segmentation. In *Advances in neural information processing systems*, pages 1495–1503, 2015.
- [9] Tao Hu, Pengwan Yang, Chilian Zhang, Gang Yu, Yadong Mu, and Cees GM Snoek. Attention-based multi-context

- guiding for few-shot semantic segmentation. In *Proceedings of the AAAI Conference on Artificial Intelligence*, volume 33, pages 8441–8448, 2019.
- [10] Wei-Chih Hung, Yi-Hsuan Tsai, Yan-Ting Liou, Yen-Yu Lin, and Ming-Hsuan Yang. Adversarial learning for semi-supervised semantic segmentation. *arXiv preprint arXiv:1802.07934*, 2018.
 - [11] Xiang Jiang, Mohammad Havaei, Farshid Varno, Gabriel Chartrand, Nicolas Chapados, and Stan Matwin. Learning to learn with conditional class dependencies. In *International Conference on Learning Representations*, 2018.
 - [12] Anna Khoreva, Rodrigo Benenson, Jan Hosang, Matthias Hein, and Bernt Schiele. Simple does it: Weakly supervised instance and semantic segmentation. In *Proceedings of the IEEE conference on computer vision and pattern recognition*, pages 876–885, 2017.
 - [13] Gregory Koch, Richard Zemel, and Ruslan Salakhutdinov. Siamese neural networks for one-shot image recognition. In *ICML deep learning workshop*, volume 2. Lille, 2015.
 - [14] Tsung-Yi Lin, Michael Maire, Serge Belongie, James Hays, Pietro Perona, Deva Ramanan, Piotr Dollár, and C Lawrence Zitnick. Microsoft coco: Common objects in context. In *European conference on computer vision*, pages 740–755. Springer, 2014.
 - [15] Jonathan Long, Evan Shelhamer, and Trevor Darrell. Fully convolutional networks for semantic segmentation. In *Proceedings of the IEEE conference on computer vision and pattern recognition*, pages 3431–3440, 2015.
 - [16] Ping Luo, Guangrun Wang, Liang Lin, and Xiaogang Wang. Deep dual learning for semantic image segmentation. In *Proceedings of the IEEE International Conference on Computer Vision*, pages 2718–2726, 2017.
 - [17] Sudhanshu Mittal, Maxim Tatarchenko, and Thomas Brox. Semi-supervised semantic segmentation with high-and low-level consistency. *IEEE Transactions on Pattern Analysis and Machine Intelligence*, 2019.
 - [18] Khoi Nguyen and Sinisa Todorovic. Feature weighting and boosting for few-shot segmentation. In *Proceedings of the IEEE International Conference on Computer Vision*, pages 622–631, 2019.
 - [19] George Papandreou, Liang-Chieh Chen, Kevin P Murphy, and Alan L Yuille. Weakly-and semi-supervised learning of a deep convolutional network for semantic image segmentation. In *Proceedings of the IEEE international conference on computer vision*, pages 1742–1750, 2015.
 - [20] Adam Paszke, Sam Gross, Soumith Chintala, Gregory Chanan, Edward Yang, Zachary DeVito, Zeming Lin, Alban Desmaison, Luca Antiga, and Adam Lerer. Automatic differentiation in pytorch. 2017.
 - [21] Kate Rakelly, Evan Shelhamer, Trevor Darrell, Alyosha Efros, and Sergey Levine. Conditional networks for few-shot semantic segmentation. 2018.
 - [22] Mengye Ren, Eleni Triantafillou, Sachin Ravi, Jake Snell, Kevin Swersky, Joshua B Tenenbaum, Hugo Larochelle, and Richard S Zemel. Meta-learning for semi-supervised few-shot classification. *arXiv preprint arXiv:1803.00676*, 2018.
 - [23] Olga Russakovsky, Jia Deng, Hao Su, Jonathan Krause, Sanjeev Satheesh, Sean Ma, Zhiheng Huang, Andrej Karpathy, Aditya Khosla, Michael Bernstein, et al. Imagenet large scale visual recognition challenge. *International journal of computer vision*, 115(3):211–252, 2015.
 - [24] Amirreza Shaban, Shray Bansal, Zhen Liu, Irfan Essa, and Byron Boots. One-shot learning for semantic segmentation. *arXiv preprint arXiv:1709.03410*, 2017.
 - [25] Mennatullah Siam, Boris N Oreshkin, and Martin Jagersand. Amp: Adaptive masked proxies for few-shot segmentation. In *Proceedings of the IEEE International Conference on Computer Vision*, pages 5249–5258, 2019.
 - [26] Karen Simonyan and Andrew Zisserman. Very deep convolutional networks for large-scale image recognition. *arXiv preprint arXiv:1409.1556*, 2014.
 - [27] Jake Snell, Kevin Swersky, and Richard Zemel. Prototypical networks for few-shot learning. In *Advances in neural information processing systems*, pages 4077–4087, 2017.
 - [28] Nasim Souly, Concetto Spampinato, and Mubarak Shah. Semi supervised semantic segmentation using generative adversarial network. In *Proceedings of the IEEE International Conference on Computer Vision*, pages 5688–5696, 2017.
 - [29] Flood Sung, Yongxin Yang, Li Zhang, Tao Xiang, Philip HS Torr, and Timothy M Hospedales. Learning to compare: Relation network for few-shot learning. In *Proceedings of the IEEE Conference on Computer Vision and Pattern Recognition*, pages 1199–1208, 2018.
 - [30] Oriol Vinyals, Charles Blundell, Timothy Lillicrap, Daan Wierstra, et al. Matching networks for one shot learning. In *Advances in neural information processing systems*, pages 3630–3638, 2016.
 - [31] Kaixin Wang, Jun Hao Liew, Yingtian Zou, Daquan Zhou, and Jiashi Feng. Panet: Few-shot image semantic segmentation with prototype alignment. In *Proceedings of the IEEE International Conference on Computer Vision*, pages 9197–9206, 2019.
 - [32] Yunchao Wei, Huaxin Xiao, Honghui Shi, Zequn Jie, Jiashi Feng, and Thomas S Huang. Revisiting dilated convolution: A simple approach for weakly-and semi-supervised semantic segmentation. In *Proceedings of the IEEE Conference on Computer Vision and Pattern Recognition*, pages 7268–7277, 2018.
 - [33] Chi Zhang, Guosheng Lin, Fayao Liu, Rui Yao, and Chunhua Shen. Canet: Class-agnostic segmentation networks with iterative refinement and attentive few-shot learning. In *Proceedings of the IEEE Conference on Computer Vision and Pattern Recognition*, pages 5217–5226, 2019.
 - [34] Xiaolin Zhang, Yunchao Wei, Yi Yang, and Thomas Huang. Sg-one: Similarity guidance network for one-shot semantic segmentation. *arXiv preprint arXiv:1810.09091*, 2018.
 - [35] Hengshuang Zhao, Jianping Shi, Xiaojuan Qi, Xiaogang Wang, and Jiaya Jia. Pyramid scene parsing network. In *Proceedings of the IEEE conference on computer vision and pattern recognition*, pages 2881–2890, 2017.